

# Local orbital occupation and energy levels of Co in $\text{Na}_x\text{CoO}_2$ : A soft x-ray absorption study

H.-J. Lin,<sup>1</sup> Y. Y. Chin,<sup>1,2,3</sup> Z. Hu,<sup>3</sup> G. J. Shu,<sup>4</sup> F. C. Chou,<sup>1,4</sup> H. Ohta,<sup>5</sup> K. Yoshimura,<sup>5</sup> S. Hébert,<sup>6</sup> A. Maignan,<sup>6</sup> A. Tanaka,<sup>7</sup> L. H. Tjeng,<sup>3</sup> and C. T. Chen<sup>1</sup>

<sup>1</sup>National Synchrotron Radiation Research Center, Hsinchu 30076, Taiwan

<sup>2</sup>II. Physikalisches Institut, Universität zu Köln, Zùlpicher Str.77, 50937 Köln, Germany

<sup>3</sup>Max-Planck-Institut für Chemische Physik fester Stoffe, Nöthnitzer Str. 40, 01187 Germany

<sup>4</sup>Center for Condensed Matter Sciences, National Taiwan University, Taipei 10617, Taiwan

<sup>5</sup>Department of Chemistry, Graduate School of Science, Kyoto University, Kyoto 606-8502, Japan

<sup>6</sup>Laboratoire CRISMAT, UMR 6508, CNRS-ENSICAEN, 6 Bd. Maréchal Juin, 14050 Caen Cedex, France

<sup>7</sup>Department of Quantum Matter, ADSM, Hiroshima University, Higashi-Hiroshima 739-8530, Japan

(Received 23 September 2009; revised manuscript received 5 March 2010; published 31 March 2010)

We present a combined experimental and theoretical investigation on the orbital occupation and local symmetry of Co in  $\text{Na}_x\text{CoO}_2$ . We have carried out polarization dependent Co- $L_{2,3}$  soft x-ray absorption spectroscopy measurements. By comparing the spectra with the results of configuration-interaction cluster calculations which include the full-atomic multiplet theory, we have found that the local symmetry for the Co ions are well-described by the  $D_{3d}$  point group with intermixing between the cubic  $t_{2g}^\pm$  and  $e_g^\pm$  orbitals. We have determined that the  $t_{2g}$  holes in both the  $\text{Na}_{0.75}\text{CoO}_2$  and  $\text{Na}_{0.5}\text{CoO}_2$  compositions reside mainly in the  $a_{1g}$  orbital. The spectroscopically deduced  $\text{Co}^{4+}/\text{Co}^{3+}$  ratio agrees well with the nominal Na concentration. We discuss the surprising observation that the single-site cluster approach is still adequate to reproduce the spectra despite the mixed valent character of the Co ions in this compound.

DOI: [10.1103/PhysRevB.81.115138](https://doi.org/10.1103/PhysRevB.81.115138)

PACS number(s): 71.20.-b, 71.28.+d, 71.70.Ch, 78.70.Dm

The electronic properties of sodium cobalt oxides have attracted considerable experimental and theoretical attention in recent years since the discovery of the exceptionally high thermopower in  $\text{NaCo}_2\text{O}_4$  (Refs. 1 and 2) and superconductivity in the hydrated cobaltate  $\text{Na}_{0.35}\text{CoO}_2 \cdot 1.3\text{H}_2\text{O}$ .<sup>3</sup> This class of compounds is particularly interesting because there are parallels to be made with the high- $T_c$  copper oxide superconductors: for both type of compounds, the electrical conductivity is governed by charge carriers which move mainly in two-dimensional planes separated by insulating layers.<sup>4</sup> Yet there are also differences. The cuprates have a planar square lattice of the transition metal ions, while the sodium cobalt oxides exhibit a triangular lattice. The local coordination is also different. The  $\text{Na}_x\text{CoO}_2$  consists of alternating layers of  $\text{CoO}_2$  and Na along the  $c$  axis, in which the edge-sharing  $\text{CoO}_6$  octahedra in the  $\text{CoO}_2$  layers have their threefold (111) axis oriented parallel to the  $c$  axis and show a noticeable compression along this direction. The local point group symmetry of the Co ion is therefore close to  $D_{3d}$ .

There is a considerable debate in the literature concerning the local electronic structure of the Co ions in  $\text{Na}_x\text{CoO}_2$ , in particular, about their spin state, orbital polarization and crystal field levels.<sup>5–27</sup> Fig. 1 illustrates the relevant one-electron energy levels.<sup>28</sup> In  $O_h$  symmetry, the  $3d$  atomic states are split into the well-known  $e_g$  and  $t_{2g}$  orbitals. In  $D_{3d}$  symmetry, the  $t_{2g}$  states are further split into a two-fold degenerate  $e_g^\pi$  and a nondegenerate  $a_{1g}$ , while the  $e_g$  states remain doubly degenerated, now called  $e_g^\sigma$ . Earlier studies suggested a low-spin (LS) state for both the  $\text{Co}^{3+}3d^6$  ion ( $S=0$ ) and the  $\text{Co}^{4+}3d^5$  ( $S=1/2$ ) in the  $\text{Na}_x\text{CoO}_2$  system.<sup>5,7,8</sup> Based on optical conductivity data of  $\text{Na}_{0.82}\text{CoO}_2$ , however, Bernhard *et al.* proposed that, following the formation of the  $\text{Co}^{3+}/\text{Co}^{4+}$  charge ordering state, the  $\text{Co}^{4+}$  ion would drive a displacement of the neighboring oxygens towards itself and thus cause a local symmetry lower than  $D_{3d}$  for its adjacent  $\text{Co}^{3+}$  ions.<sup>6</sup> They concluded that this mechanism would lead

to a further splitting of the  $e_g^\sigma$  doublet and stabilizes the intermediate-spin (IS) state with  $S=1$ . Moreover, a subsequent theoretical spin-orbital-polaron model supported the IS state for  $\text{Co}^{3+}$  in the  $\text{Na}_x\text{CoO}_2$  at large  $x$ , i.e., small hole concentrations,<sup>9</sup> with a local symmetry lower than  $D_{3d}$ . A recent polarization dependent soft x-ray absorption (XAS) experiment and a theoretical analysis thereof<sup>10,11</sup> claimed also to have observed the presence of appreciable crystal fields with a symmetry lower than  $D_{3d}$ , yet they supported the LS and not the IS scenario. It was also concluded, however, that the samples used in these XAS studies showed  $\text{Co}^{3+}/\text{Co}^{4+}$  spectral ratios which were inconsistent with their nominal Na contents.

Here we report our investigation on the local electronic structure of  $\text{Na}_x\text{CoO}_2$  using polarization dependent XAS experiments at the Co  $L_{2,3}$  edges in combination with detailed full-multiplet cluster model calculations. We found that the  $\text{Co}^{3+}/\text{Co}^{4+}$  spectral contents do match the nominal Na concentration and that the spectral features can be excellently

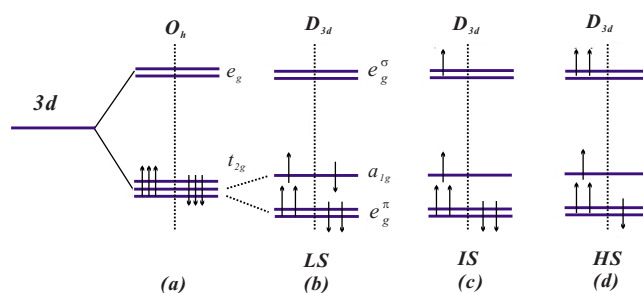


FIG. 1. (Color online) Schematic one-electron energy level diagram for a  $\text{Co}^{3+}3d^6$  ion: (a) in  $O_h$  symmetry with low-spin configuration; (b)  $D_{3d}$  symmetry, low spin; (c)  $D_{3d}$ , intermediate spin; (d)  $D_{3d}$ , high spin. For a  $\text{Co}^{4+}3d^5$  ion, one spin down electron is removed from each diagram.

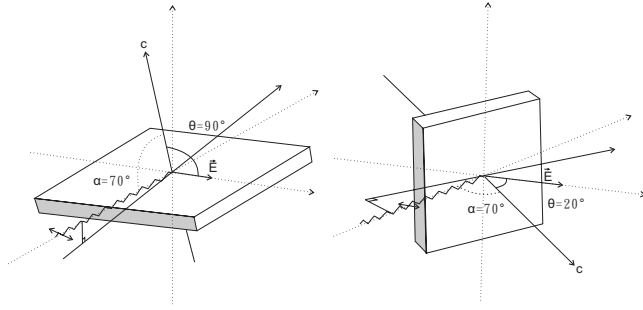


FIG. 2. Experimental geometry with polarization of the light in the horizontal plane.  $\theta$  is the angle between the electric field vector  $\vec{E}$  and the  $c$ -axis surface normal, and  $\alpha$  the tilt between the Poynting vector and the surface normal.

described using the  $D_{3d}$  local symmetry for the Co ions. We are also able to obtain quantitative estimates for the orbital polarization of the charge carriers.

Single crystals of various Na concentrations were prepared from  $\text{Na}_{0.82}\text{CoO}_2$  through subsequent electrochemical deintercalation procedures. Details of the crystal growth are described elsewhere.<sup>29,30</sup> The XAS experiments were carried out at the dragon beamline of the National Synchrotron Radiation Research Center (NSRRC) in Taiwan. The photon energy resolution at the Co  $L_{2,3}$  edges ( $h\nu \approx 770\text{--}800$  eV) was set at 0.3 eV. The degree of linear polarization of the incident light was  $\sim 99\%$ . The spectra were recorded using the total electron yield method and a CoO single crystal was measured simultaneously in a separate chamber to calibrate the photon energy with an accuracy better than 0.01 eV for all polarization dependent measurements. Clean sample surfaces were obtained by cleaving the single crystals *in situ* at pressures in the low  $10^{-10}$  mbar range.

The samples were tilted with respect to the incoming beam, so that the Poynting vector of the light makes an angle of  $\alpha = 70^\circ$  with respect to the  $c$ -axis surface normal. To change the polarization, the sample was rotated around the Poynting vector axis as depicted in Fig. 2, and  $\theta$ , the angle between the electric-field vector  $\vec{E}$  and the  $c$  axis, can be varied between  $20^\circ$  and  $90^\circ$ . This measurement geometry allows for an optical path of the incoming beam which is independent of  $\theta$ , which guarantees a reliable comparison of the spectral line shapes as a function of polarization. The spectra for the electric field vector  $\vec{E}$  parallel to the  $c$  axis can be obtained from the measured data by using the formula,  $I_{\parallel} = [I_{ip} - I_{\perp} \cos^2(\alpha)] / \sin^2(\alpha)$ , where  $I_{ip}$  and  $I_{\perp}$  are the measured intensities with  $\theta = 20^\circ$  and  $\theta = 90^\circ$ , respectively, and  $\sin^2(\alpha) = 0.883$  and  $\cos^2(\alpha) = 0.117$ . The isotropic spectra can be obtained from  $I_{\parallel} + 2 I_{\perp}$ .

Figure 3 shows the isotropic Co  $L_{2,3}$  XAS spectra of  $\text{Na}_{0.5}\text{CoO}_2$  and  $\text{Na}_{0.75}\text{CoO}_2$  taken at room temperature. We have also included the spectra of  $\text{LaCoO}_3$  (reproduced from Ref. 31) and  $\text{BaCoO}_3$ . The displayed  $\text{LaCoO}_3$  spectrum is the one measured in the low-temperature phase and serves as a reference for a LS  $\text{Co}^{3+}$  system.<sup>31</sup> Analogously, the  $\text{BaCoO}_3$  is taken here as a reference for a LS  $\text{Co}^{4+}$  system.<sup>32</sup> For the  $\text{BaCoO}_3$  spectrum we have removed the Ba  $M_{4,5}$  white lines located at 784 and 798 eV energies using the Ba  $M_{4,5}$  spectrum of  $\text{BaFeO}_3$ .<sup>32</sup> To facilitate the following discussion, the

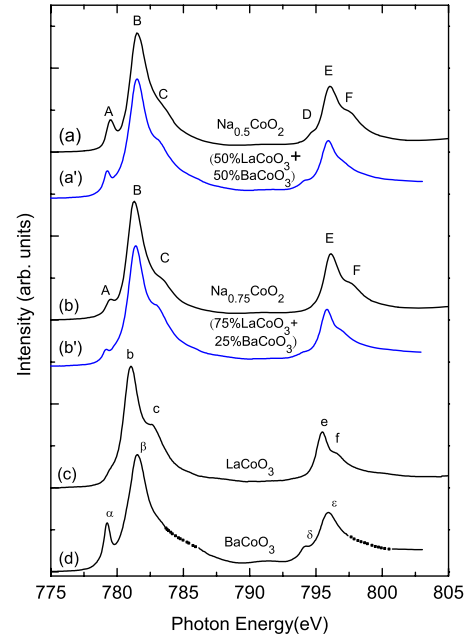


FIG. 3. (Color online) Experimental isotropic Co  $L_{2,3}$  XAS spectra of (a)  $\text{Na}_{0.5}\text{CoO}_2$ , (b)  $\text{Na}_{0.75}\text{CoO}_2$ , (c)  $\text{LaCoO}_3$  ( $\text{Co}^{3+}$ ) in the low-spin phase, and (d)  $\text{BaCoO}_3$  ( $\text{Co}^{4+}$ ). Composite spectra of (a') 50%  $\text{LaCoO}_3$  plus 50%  $\text{BaCoO}_3$  and (b') 0.75%  $\text{LaCoO}_3$  plus 25%  $\text{BaCoO}_3$ .

$\text{LaCoO}_3$  and  $\text{BaCoO}_3$  spectra shown in Fig. 3 have been shifted by 0.6 eV and  $-0.4$  eV, respectively, in energy.

The spectra are dominated by the Co  $2p$  core-hole spin-orbit coupling, which split the spectrum roughly into two parts, namely, the  $L_3$  ( $h\nu \approx 782$  eV) and  $L_2$  ( $h\nu \approx 797$  eV) white line regions. The lineshape of the spectrum depends strongly on the multiplet structure given by the atomiclike Co  $2p\text{--}3d$  and  $3d\text{--}3d$  Coulomb and exchange interactions, as well as by the solid including local crystal fields and hybridization with the oxygen ligands. In the  $\text{Na}_{0.5}\text{CoO}_2$  and  $\text{Na}_{0.75}\text{CoO}_2$  spectra we can observe distinct features which we label as A-B-C in the  $L_3$  region, and D-E-F in the  $L_2$ .

To help identify the origin of these features, we now turn our attention to the spectra of the reference materials  $\text{LaCoO}_3$  and  $\text{BaCoO}_3$ . There we can see that a LS  $\text{Co}^{3+}$  has structures b-c and e-f resembling the  $\text{Na}_x\text{CoO}_2$  B-C and E-F, respectively, while a LS  $\text{Co}^{4+}$  has peaks  $\alpha\text{--}\beta$  and  $\delta\text{--}\epsilon$  very similar to the  $\text{Na}_x\text{CoO}_2$  A-B and D-E, respectively. This strongly suggests that features A and D in the sodium cobaltates are pure signatures of the  $\text{Co}^{4+}$  component, while C and F are due to the  $\text{Co}^{3+}$ . Peaks B and E, on the other hand, have contributions from both the  $\text{Co}^{3+}$  and  $\text{Co}^{4+}$ . The assignment of peak A to  $\text{Co}^{4+}$  is consistent with the observation that its intensity decreases in going from  $\text{Na}_{0.5}\text{CoO}_2$  to  $\text{Na}_{0.75}\text{CoO}_2$ . The same is also the case for peak D. It becomes even too weak to be visible in the  $x=0.75$  spectrum.

As an *ansatz* for further confirmation, we have made composite spectra consisting of 50%  $\text{LaCoO}_3$  plus 50%  $\text{BaCoO}_3$  and 75%  $\text{LaCoO}_3$  plus 25%  $\text{BaCoO}_3$ . In doing this we have shifted the  $\text{LaCoO}_3$  and  $\text{BaCoO}_3$  slightly as already mentioned above. We would like to note that it is an experimental observation to have compounds showing slight energy differ-

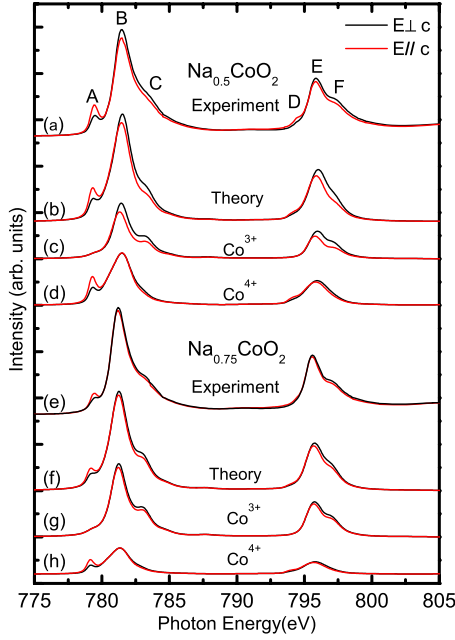


FIG. 4. (Color online) Polarization dependent Co  $L_{2,3}$  XAS spectra of  $\text{Na}_{0.5}\text{CoO}_2$  and  $\text{Na}_{0.75}\text{CoO}_2$ . (a) and (e) are the experimental spectra; (b)–(d) and (f)–(h) are the corresponding theoretical spectra together with their respective  $\text{Co}^{3+}$  and  $\text{Co}^{4+}$  contributions.

ences despite the fact that they have the same valence and we ascribe this to differences in the screening during the XAS process associated with differences in the local and extended environment of the ions in the compounds. We can see from curves (a') and (b') in Fig. 3 that these composite spectra reproduce reasonable well those of  $\text{Na}_{0.5}\text{CoO}_2$  and  $\text{Na}_{0.75}\text{CoO}_2$ , suggesting that the  $\text{Co}^{3+}/\text{Co}^{4+}$  spectral contents are quite consistent with the nominal Na concentrations. In fact, these experimental findings falsify the peak assignments made in the recent XAS study<sup>10,11</sup> mentioned above and thus also their claim concerning the improper Na concentration in their samples.

In our attempt to interpret the isotropic spectra of the sodium cobaltates, we note first of all that the match with the composite spectra of the  $\text{LaCoO}_3$  and  $\text{BaCoO}_3$  as described above is very reasonable but not perfect. This is not surprising since it simply indicates that the local and extended coordination of the Co ions in the three types of compounds is sufficiently different to cause observable differences in, e.g., the crystal field and Madelung parameters. To obtain more detailed information about the local electronic structure of the sodium cobaltates we now will make use of the polarization dependence of the spectra. Figure 4 shows the Co  $L_{2,3}$  XAS spectra of  $\text{Na}_{0.5}\text{CoO}_2$  (curve a) and  $\text{Na}_{0.75}\text{CoO}_2$  (curve e) for  $E \perp c$  and  $E \parallel c$ . We can clearly observe that there is a pronounced polarization dependence and that this so-called linear dichroic effect is stronger for the  $x=0.5$  composition than for the  $x=0.75$ . This directly suggests that the hole-like charge carriers are orbitally very anisotropic.

To extract the information concerning the orbital occupation and level splittings, we will analyze the  $L_{2,3}$  XAS spectra and the linear dichroism therein using the configuration-interaction cluster model that includes the full-atomic

multiplet theory and the hybridization of the central transition metal ion with the O  $2p$  ligands.<sup>33,34</sup> This approach has been successfully applied for a wide range of correlated oxides, including various Co oxide materials.<sup>31,35–40</sup> Crystal structure data<sup>41</sup> reveal that the local coordination of the Co ions can be well approximated by a  $\text{CoO}_6$  cluster in  $D_{3d}$  point group. We will use this cluster in our calculations with the XTLS 8.3 code.<sup>34</sup>

In the simulations for the  $\text{Co}^{3+}$  site we started with the parameter values found for  $\text{LiCoO}_2$ ,<sup>42,43</sup> a compound having the  $\text{Co}^{3+}$  ions arranged also in a triangular lattice. These parameter values are very close to those of  $\text{LaCoO}_3$ ,<sup>31,44–50</sup> except that here the O  $2p$  to Co  $3d$  charge transfer energy  $\Delta^{3+}$  is about 4 eV instead of about 2 eV, a finding which is probably related to a difference in the Madelung potential associated with the different arrangement of the Co ions in the crystal. For the  $\text{Co}^{4+}$  site we use a charge-transfer energy  $\Delta^{4+}$  of  $-1$  eV as determined by the relation  $\Delta^{4+} = \Delta^{3+} - U_{dd}$  with  $U_{dd} = 5$  eV.<sup>31,35,37,40,44–46</sup> A summary of the parameter values is listed in Ref. 51. In the calculations we have tuned only the trigonal crystal-field parameters<sup>28</sup>  $D\sigma$  and  $D\tau$  as to obtain the best simulation of the experimental spectra. In the calculations, we have used slightly different optimal parameter values for the two different compositions as we will describe below in more detail.

The results of the simulations are depicted in Fig. 4. We can observe that we are able to obtain excellent simulations of the experimental spectra. Also here we have made composite spectra consisting of incoherent sums of 50%  $\text{Co}^{3+}$  plus 50%  $\text{Co}^{4+}$  and 75%  $\text{Co}^{3+}$  plus 25%  $\text{Co}^{4+}$  to reproduce the  $\text{Na}_{0.5}\text{CoO}_2$  and  $\text{Na}_{0.75}\text{CoO}_2$  spectra, respectively. The excellence of the fits indicates first of all that we have obtained a reasonable detailed understanding of the local electronic structure. It also demonstrates that a strict  $D_{3d}$  local symmetry for both  $\text{Co}^{3+}$  and  $\text{Co}^{4+}$  ions is sufficient to explain the observed spectral features and polarization dependence, refuting the need for a local symmetry lower than  $D_{3d}$  for the  $\text{Co}^{3+}$  ion as claimed previously.<sup>11</sup> Moreover, the fact that the  $\text{Co}^{3+}/\text{Co}^{4+}$  spectral fractions used to reproduce the spectra matches the nominal Na concentrations also indicates that the samples are of proper stoichiometry. We note that the separate  $\text{Co}^{3+}$  and  $\text{Co}^{4+}$  simulations also match reasonably well those of  $\text{LaCoO}_3$  and  $\text{BaCoO}_3$ , respectively, justifying our approach in Fig. 3 to explain the sodium cobaltate spectra using these two reference compounds.

Let us analyze the origin of the polarization dependence in the XAS spectra of  $\text{Na}_x\text{CoO}_2$ . In the absence of the trigonal crystal field, the  $t_{2g}$  eigenstates of the  $O_h$  point group can be rewritten as  $a_{1g} = d_{3z^2-y^2}$ ,  $t_{2g}^+ = \sqrt{2/3}d_{x^2-y^2} - \sqrt{1/3}d_{xz}$ , and  $t_{2g}^- = \sqrt{2/3}d_{xy} + \sqrt{1/3}d_{yz}$ , while the  $e_g$  as  $e_g^+ = \sqrt{1/3}d_{x^2-y^2} + \sqrt{2/3}d_{xz}$  and  $e_g^- = \sqrt{1/3}d_{xy} - \sqrt{2/3}d_{yz}$ , where the  $z$  axis is now defined along the  $c$  axis of the  $D_{3d}$  point group. A nonzero value of the trigonal crystal-field parameters  $D\sigma$  and  $D\tau$  will lead to the formation of  $a_{1g}$ ,  $e_g^\pi$ , and  $e_g^\sigma$  eigenstates of the  $D_{3d}$  mentioned above. In order to facilitate the discussion, we re-express the parameters  $D\sigma$  and  $D\tau$  in terms of  $D_{trig}^0$  and  $V_{mix}$ .  $D_{trig}^0 = -3D\sigma - 20D\tau/3$  is the crystal-field splitting between the  $a_{1g}$  and the  $t_{2g}^\pm$  orbitals. It is defined as positive when the  $a_{1g}$  orbital is higher in energy (more unstable) than the  $t_{2g}^\pm$ .  $V_{mix} = \sqrt{2}D\sigma - 5\sqrt{2}D\tau/3$  describes the mixing between



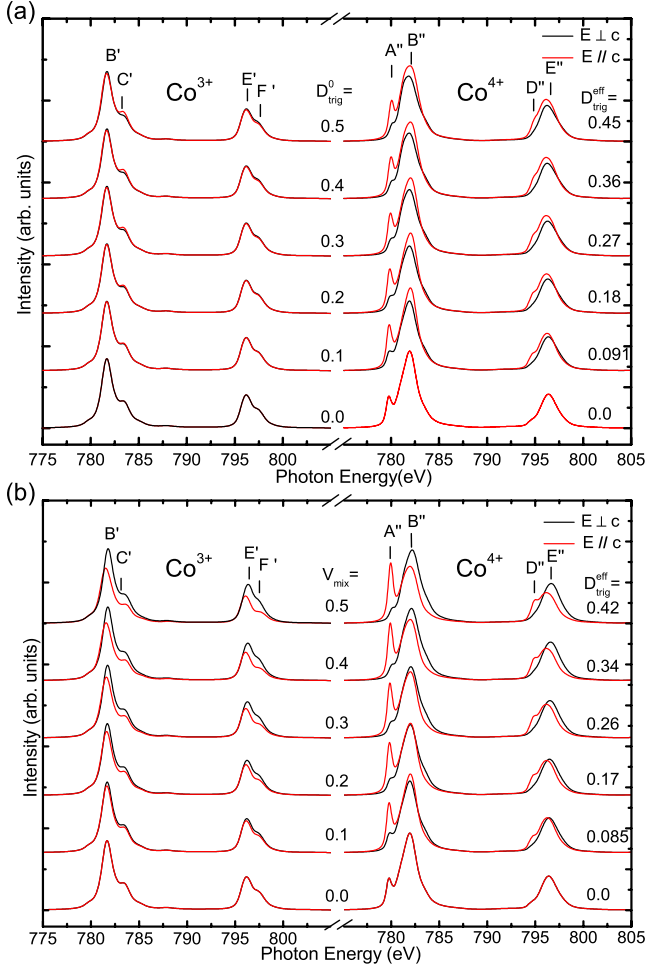


FIG. 5. (Color online) Calculated polarization dependent Co  $L_{2,3}$  XAS spectra of  $\text{Co}^{3+}$  (left) and  $\text{Co}^{4+}$  (right) as a function of the bare trigonal crystal field splitting  $D_{\text{trig}}^0$  (top panel a) and as a function of the mixing parameter  $V_{\text{mix}}$  in  $D_{3d}$  symmetry. See text for definitions of  $D_{\text{trig}}^0$  and  $V_{\text{mix}}$ .

the  $t_{2g}^{\pm}$  and  $e_g^{\pm}$ , i.e.,  $V_{\text{mix}} = \langle t_{2g}^{\pm} | H | e_g^{\pm} \rangle$ , leading to the formation of the  $e_g^{\pi}$  and the  $e_g^{\sigma}$  orbitals. We will call  $D_{\text{trig}}^0$  the bare trigonal crystal-field splitting between the  $a_{1g}$  and  $e_g^{\pi}$  orbitals: bare because the splitting is taken without the energy stabilization of the  $e_g^{\pi}$  orbital due to the mixing of the  $t_{2g}^{\pm}$  with the higher lying  $e_g^{\sigma}$  orbitals. We will further define one more quantity, namely,  $D_{\text{trig}}^{\text{eff}}$ , which represents the effective  $a_{1g}-e_g^{\pi}$  splitting for the  $\text{Co}^{4+}$  cluster after including the  $t_{2g}^{\pm}-e_g^{\sigma}$  mixing and the hybridization with the oxygen ligands. This quantity can be read directly from the  $\text{Co}^{4+}$  total energy diagram calculated with the Co  $3d$  spin-orbit interaction switched off.

Figure 5 panel (a) shows the polarization dependence for the  $\text{Co}^{3+}$  site (left) and the  $\text{Co}^{4+}$  (right) as a function of the bare trigonal crystal field  $D_{\text{trig}}^0$ . Starting with the spectrum for the  $\text{Co}^{3+}$ , it is evident that there is no polarization dependence when the trigonal crystal field is absent since in this effectively  $O_h$  symmetry the electronic configuration for this low spin  $\text{Co}^{3+}$  is a highly symmetric closed shell  $3d^6 t_{2g}^6$ . The peaks B', C', E', and F' can be assigned to transitions from the  $2p_{3/2}$  and  $2p_{1/2}$  core to the empty  $3d e_g$  orbitals. The

splitting between B' and C', as well as between E' and F', is a multiplet effect as explained in a previous theoretical work.<sup>52</sup>

Upon switching on  $D_{\text{trig}}^0$ , one can observe the occurrence of some linear dichroism for the  $\text{Co}^{3+}$ : the intensities of peaks B' and E' become a function of the polarization and also the positions of peaks B' and E' are somewhat polarization dependent. These tiny energy shifts in the peak positions reflect directly the splitting within the  $e_g$  orbitals. Nevertheless, the main conclusion which one can draw from this figure is that  $D_{\text{trig}}^0$  induces only a very small linear dichroic effect in the  $\text{Co}^{3+}$  spectrum. All this is consistent with the fact that the  $^1A_1$  ground-state symmetry of the LS  $\text{Co}^{3+}$  is not split by these bare trigonal crystal fields.

We now focus on the polarization dependence of the  $\text{Co}^{4+}$  due to the bare trigonal crystal field. We start first with the  $D_{\text{trig}}^0 = 0$  case, for which there is no dichroism to be observed. In comparison to a  $\text{Co}^{3+}3d^6$  ion, the  $\text{Co}^{4+}3d^5$  has the additional low lying peaks labelled A'' and D''. These reflect the presence of a hole in the  $t_{2g}$  subshell, giving an extra channel into which a  $2p_{3/2}$  or a  $2p_{1/2}$  core electron, respectively, can be excited during the XAS transition. This hole is isotropically distributed over the  $a_{1g}$  and  $t_{2g}^{\pm}$  orbitals in this effectively  $O_h$  surrounding. Upon switching on  $D_{\text{trig}}^0$ , one can make the striking observation from the curves on the right of panel (a) in Fig. 5 that already a small value of  $D_{\text{trig}}^0$  is sufficient to generate a pronounced linear dichroism in peaks A'' and D''. The dichroic effect here, defined as the intensity difference for the two polarizations, is very much larger than for the  $\text{Co}^{3+}$ .

A detailed look given in panel (a) of Fig. 6 reveals in fact, that after an initially rapid increase, the dichroic effect reaches a high but rather constant value as a function of  $D_{\text{trig}}^0$  or  $D_{\text{trig}}^{\text{eff}}$  (these two quantities are practically equal, i.e., they differ by less than 10%—see the legends on the right in panel (a) of Fig. 5. This can be understood as follows. The introduction of a positive  $D_{\text{trig}}^0$  and consequently, a positive  $D_{\text{trig}}^{\text{eff}}$ , leads to the unoccupation of the minority-spin  $a_{1g}$  orbital. Since the  $a_{1g}$  wave function is also highly directional, this leads naturally to the very strong polarization dependence of the probability with which the Co  $2p \rightarrow 3d$  transition occurs.<sup>53</sup> Here we note that in getting the  $a_{1g}$  orbital unoccupied,  $D_{\text{trig}}^{\text{eff}}$  has to compete with the Co  $3d$  spin-orbit interaction, which mixes the  $a_{1g}$  with the  $e_g^{\pi}$  orbitals. In other words,  $D_{\text{trig}}^{\text{eff}}$  has to be large enough as to lift the mixing of these orbitals. This explains why the linear dichroism reaches its largest asymptotic values only for  $D_{\text{trig}}^{\text{eff}}$  exceeding about 80 meV, which is the strength of the  $3d$  spin-orbit interaction.<sup>54</sup>

Next, we investigate the influence of  $V_{\text{mix}}$  on the spectra. The results are depicted in panel (b) of Fig. 5: the curves on the left are for the  $\text{Co}^{3+}$  and on the right for the  $\text{Co}^{4+}$ . The calculations were done for  $V_{\text{mix}}$  ranging from 0 to 0.5 eV, with  $D_{\text{trig}}^0$  set to zero. For the  $\text{Co}^{3+}$  we can clearly observe a strong polarization dependence for peaks B', C', E', and F'. The dichroic effect scales rather linearly with  $V_{\text{mix}}$  as depicted more clearly for peak B' in Fig. 6. The origin of this lies in the fact that the mixing between the cubic  $t_{2g}^{\pm}$  and  $e_g^{\sigma}$  wave functions results in the formation of the noncubic  $e_g^{\pi}$

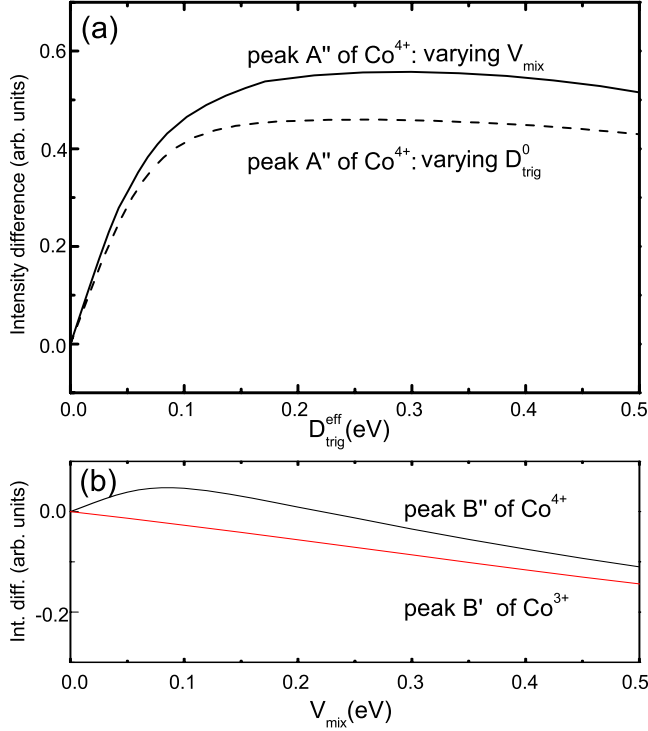


FIG. 6. (Color online) Panel (a): Intensity difference between the  $\mathbf{E} \perp \mathbf{c}$  and  $\mathbf{E} \parallel \mathbf{c}$  alignments for peak A'' in the calculated  $Co^{4+}$  spectra as a function of  $D_{trig}^{eff}$ . Panel (b): *idem* for peak B'' of the  $Co^{4+}$  and peak B' of the  $Co^{3+}$  as a function of  $V_{mix}$ .

and the  $e_g^\sigma$  orbitals.<sup>28</sup> This changes the ground state of the low spin  $Co^{3+}$  system from the highly symmetric formally closed shell  $t_{2g}^6$  configuration into a state in which the electron distribution is anisotropic: a positive  $V_{mix}$  makes the occupied  $e_g^\pi$  to be directed more along the  $c$  axis and unoccupied the  $e_g^\sigma$  more into the  $a-b$  plane, which is reflected by the higher absorption intensity for  $\mathbf{E} \perp \mathbf{c}$  as compared to  $\mathbf{E} \parallel \mathbf{c}$  as shown by the left curves in panel (b) of Fig. 5.

The effect of  $V_{mix}$  for the  $Co^{4+}$  is also very large. The spectral changes are more complicated: here the polarization dependence of peaks A'' and D'' is the same as that of peaks B'' and E'' for small  $V_{mix}$  values, but becomes opposite for large  $V_{mix}$  numbers. To understand this result we also have calculated  $D_{trig}^{eff}$ , the effective  $a_{1g}-e_g^\pi$  splitting, as indicated by the legends next to the curves on the right in panel (b) of Fig. 5. Please note that this effective splitting here is caused by  $V_{mix}$  only, since  $D_{trig}^0$  is set to zero; in other words, we see here the stabilization of the  $e_g^\pi$  orbitals with respect to the  $a_{1g}$  due to the mixing of these  $e_g^\pi$  orbitals with the higher lying  $e_g^\sigma$ . We then plot the linear dichroic effect for peak A'' as a function of  $D_{trig}^{eff}$  in panel (a) of Fig. 6, and observe a very similar behavior as when the linear dichroism was induced by  $D_{trig}^0$  as discussed above. This is enlightening since  $D_{trig}^{eff}$  reflects how much the  $a_{1g}$  is more unstable than the  $e_g^\pi$  orbital, the curves in Fig. 6 basically show that the linear dichroism in peak A'' can be rather directly linked to the hole occupation in the  $a_{1g}$  orbital, no matter whether the dichroism is caused by  $D_{trig}^0$  or  $V_{mix}$  or a combination of these.

Concerning the linear dichroism in peak B'' of the  $Co^{4+}$  we now can infer the following picture: the presence of  $V_{mix}$

induces two effects, namely the unoccupation of the  $a_{1g}$  orbital giving the dichroism as can be seen for peak B'' (and A'') due to  $D_{trig}^0$  [see curves on the right of panel (a) in Fig. 5], and the redistribution of the electron density between the cubic  $t_{2g}^\pm$  and  $e_g^\pm$  wave functions leading to the formation of the noncubic  $e_g^\pi$  and the  $e_g^\sigma$  like in the case of peak B' of the  $Co^{3+}$  [see curves on the left of panel (b) in Fig. 5]. These two dichroic signals have opposite signs, and for large values of  $V_{mix}$  the latter wins, explaining the nonmonotonic behavior of the net dichroic signal in the  $Co^{4+}$  B'' peak as depicted in panel (b) of Fig. 6.

The results of Figs. 5 and 6 give us a clear strategy for how to determine the trigonal crystal-field parameters. By fitting the dichroism in the calculated peak A'' to the experimental one in peak A (see Fig. 4), we can obtain a reliable estimate for  $D_{trig}^{eff}$ . The value for  $V_{mix}$  can be fixed from fitting the dichroism in the calculated peaks B' and B'' to the experimental signal in peak B (see Fig. 4). Since  $D_{trig}^{eff}$  is determined by a combination of  $D_{trig}^0$  and  $V_{mix}$ , we then also have pinpointed the value for  $D_{trig}^0$ .

We found for the  $Na_{0.75}CoO_2$  composition that  $D_{trig}^{eff} = 0.027$  eV,  $V_{mix} = 0.1$  eV and  $D_{trig}^0 = -0.065$  eV ( $D\sigma = 0.050$  eV and  $D\tau = -0.013$  eV). Here we have used the same crystal-field parameters for the  $Co^{3+}$  and  $Co^{4+}$  sites since there is no experimental indication available to suggest that the two sites are different, i.e., the system is metallic and there is no charge ordering observed. For the  $Na_{0.5}CoO_2$  we have obtained essentially the same parameter values, except for  $V_{mix} = 0.3$  eV for the  $Co^{3+}$  ( $D\sigma = 0.13$  eV and  $D\tau = -0.050$  eV). Here we found the 3+ site to be slightly different from the 4+, not inconsistent with the experimentally observed presence of charge ordering in this insulating compound.<sup>41</sup>

It was claimed in a recent polarization dependent XAS study that there is a need for a local symmetry lower than  $D_{3d}$  for the  $Co^{3+}$  ion to explain the spectra.<sup>10,11</sup> However, the authors were still using cubic wave functions in their  $Co^{3+}$  simulations in  $D_{3d}$  symmetry, thus essentially neglecting the anisotropic mixing between  $t_{2g}$  with the  $e_g$  states due to the presence of the trigonal crystal field.<sup>28</sup> It is this mixing which is responsible for the polarization dependence in peak B'. Using the proper wave functions and full multiplet theory we are able to reproduce the polarization dependent XAS spectra in detail as we have shown above.

Interestingly, the existence of lower than  $D_{3d}$  symmetry has been also proposed from optical spectroscopy, but then only for compositions and temperatures for which a charge-ordered state appears.<sup>6</sup> This proposal need not to be inconsistent with our results. It is conceivable that the optical features appearing only in the charged ordered state are indeed caused by low symmetry crystal fields but these then must have a very small strength in comparison to that of the trigonal crystal field, so that in XAS the spectral intensities associated with the trigonal crystal field overwhelm or dominate over the possible low-symmetry features. Yet, the claimed stabilization of the IS state of the  $Co^{3+}$  ions in the charge-ordered state<sup>6</sup> cannot be evidenced from our present XAS study.

There is a considerable discussion in the literature concerning the values (and even the sign) for the trigonal

crystal-field parameters.<sup>7,10–27</sup> The negative value we found for  $D_{trig}^0$ , the bare trigonal crystal-field splitting, seems to be consistent with the expectation that point charges for an octahedron compressed along the (111) axis will stabilize the  $a_{1g}$  orbital with respect to the  $e_g^\pi$ .<sup>7,13,21</sup> Our finding for the presence of  $V_{mix}$  and corresponding destabilization of the  $a_{1g}$  orbital is an aspect which was also mentioned in some of the theoretical reports.<sup>27</sup> Yet, the net result of these two opposing effects, namely, that  $D_{trig}^{eff}$  in our study is positive, should not be taken as evidence that the centroid of the  $a_{1g}$  band is indeed higher in energy than that of the  $e_g^\pi$ . The analysis we have made here is based on a single-site cluster method which does not take into account the band formation. A positively valued  $D_{trig}^{eff}$  merely means that there is more holes in the  $a_{1g}$  than in the  $e_g^\pi$  orbitals. This can be achieved even in the case that the centroid of the  $a_{1g}$  is lower than that of the  $e_g^\pi$ , provided that the top of the partially emptied  $t_{2g}$  band has more  $a_{1g}$  than  $e_g^\pi$  character.<sup>12,17,22,27</sup>

Yet, we can provide an explicit determination of the orbital polarization of the  $t_{2g}$  holes. From the cluster calculations which yield the excellent simulation of the experimental polarization dependent spectra (see Fig. 4) we find that the  $Co^{4+}$  has about 0.58 hole in the  $a_{1g}$  orbital and 0.42 in the  $e_g^\pi$ . These numbers apply for both the  $Na_{0.5}CoO_2$  and the  $Na_{0.75}CoO_2$  compositions. Band-structure calculations<sup>12,17,27</sup> predict that for low  $x$  contents, i.e.,  $x < 0.67$ , the  $t_{2g}$  hole has indeed a mixed  $a_{1g}$  and  $e_g^\pi$  character. However, for high  $x$  contents, i.e.,  $0.67 < x < 1$ , the hole should reside only in the  $a_{1g}$  band. This is in contradiction with our findings. If the hole were of pure  $a_{1g}$  character, the linear dichroism of peak A would have been larger by a factor of 2–3 than experimentally observed. At the moment it is not clear how to reconcile this disagreement. One possibility is that the band-structure calculations reported so far in the literature did not take into account the Co 3d spin-orbit interaction, which otherwise would have resulted in a mixing between the  $a_{1g}$  and  $e_g^\pi$  bands.

Another important aspect of our polarization dependent XAS work is that we found good agreement between the  $Co^{3+}/Co^{4+}$  spectral intensity ratios and the nominal Na concentration. In the earlier study,<sup>10,11</sup> however, it was claimed that the spectroscopic data are not consistent with the specified Na content. This is quite puzzling since the experimental method is the same. We therefore set out to look into the details of that analysis and we have found that this is mainly due to the neglect in that earlier study of the Co  $2p-3d$  exchange interaction when carrying out the simulations. The consequence of such a neglect is that peaks C' and F' in the calculated  $Co^{3+}$  spectrum disappear (while in our simulations they are clearly present, see Figs. 4 and 5). The authors of that earlier study then had to attribute the experimentally observed peak C to a feature of the  $Co^{4+}$  ion. They used an unrealistic large value for the O  $2p$  to Co  $3d$  transfer integral, in order to position what is peak B'' in our calculations (see Fig. 5) at the energy of the experimental peak C. The final result is that all of the  $L_3$  intensity of their simulated  $Co^{4+}$  ion is concentrated at the energies of the experimental peaks A and C. It is then of no surprise that peak C in their theoretical spectrum has too much intensity than that found experimentally: for  $Na_{0.4}CoO_2$  they found that the calculated

feature C has twice the weight than the experimental one. They attributed this discrepancy erroneously to a proportionally lower  $Co^{4+}$  fraction than expected on the basis of the nominal Na content.

Although satisfactory, our finding that the  $Co^{3+}/Co^{4+}$  spectral intensity ratio corresponds well with the nominal Na content is also surprising. The simulations in Fig. 3 were done by constructing the composite spectra as an *incoherently* weighted sum of the  $Co^{3+}$  and  $Co^{4+}$  contributions. In principle this summation has to be done *coherently* as also argued in the earlier XAS study.<sup>11</sup> In a mixed valent situation such as we have for the  $Na_xCoO_2$  case, the spectral intensities of the  $Co^{3+}$  and  $Co^{4+}$  constituents could be appreciably redistributed in favor for the lowest lying spectral features. An example for such a redistribution process can be found for instance in the photoemission and inverse-photoemission spectra of strongly correlated insulators upon doping.<sup>55,56</sup>

Thus the fact that this does not occur in the XAS spectra of  $Na_xCoO_2$  is quite extraordinary, especially since this system is metallic with appreciable spectral weight at the Fermi level.<sup>57–60</sup> The ground state of  $Na_xCoO_2$  is therefore a coherent state of all  $Co^{3+}$  and  $Co^{4+}$  present in the lattice. Yet, the solution for this paradox may be found in the energetics of the different XAS final states which have to be compared to the one-electron nearest-neighbor hopping integrals. It is a well-known that XAS spectra are highly sensitive to the valence state: an increase in the valence state of the metal ion by one causes a shift of the XAS  $L_{2,3}$  spectra by one or more eV towards higher energies.<sup>38,61,62</sup> This shift is due to a final state effect in the x-ray absorption process. The energy difference between the XAS final states of a  $3d^n$  ( $3d^6$  for  $Co^{3+}$ ) and a  $3d^{n-1}$  ( $3d^5$  for  $Co^{4+}$ ) configuration is  $\Delta E = E(2p^6 3d^{n-1} \rightarrow 2p^5 3d^n) - E(2p^6 3d^n \rightarrow 2p^5 3d^{n+1}) \approx U_{pd} - U_{dd}$ , where  $U_{dd}$  is the Coulomb energy between two 3d electrons and  $U_{pd}$  the one between a 3d electron and the 2p core hole. Experimentally  $U_{pd} - U_{dd}$  is found to be  $\approx 1 \sim 2$  eV. On the other hand, the one-electron nearest-neighbor hopping integrals in this triangular lattice system are much smaller, especially the ones for the  $a_{1g}$  hole. Tight-binding fits<sup>21</sup> to the band-structure results<sup>12</sup> yield numbers less than 0.1 eV. This implies that the  $Co^{3+}$  and  $Co^{4+}$  XAS final states hardly mix with each other. Their intensities are then simply given by their population numbers in the coherent ground state, which in turn is determined by the Na concentration, as we have observed in our work.

In conclusion, we have carried out a detailed experimental and theoretical study on the polarization dependence of the Co- $L_{2,3}$  soft x-ray absorption spectra of  $Na_{0.5}CoO_2$  and  $Na_{0.75}CoO_2$ . We found that the  $t_{2g}$  holes have mainly an  $a_{1g}$  character. Yet we also observed a non-negligible  $e_g^\pi/e_g^\sigma$  signature, which is surprising especially for  $Na_{0.75}CoO_2$  in view of the presently available band-structure results. The data can be well explained using a local  $D_{3d}$  point group in which there is mixing between the cubic  $t_{2g}^\pm$  and  $e_g^\pm$  orbitals. The  $Co^{3+}/Co^{4+}$  spectral ratios agree well with the nominal Na concentration.

This work was supported in part by the National Science Council of Taiwan and by the Deutsche Forschungsgemeinschaft through Grant No. SFB 608 and by the European Union through the ITN SOPRANO network.



- <sup>1</sup>I. Terasaki, Y. Sasago, and K. Uchinokura, Phys. Rev. B **56**, R12685 (1997).
- <sup>2</sup>Y. Wang, N. S. Rogado, R. J. Cava, and N. P. Ong, Nature (London) **423**, 425 (2003).
- <sup>3</sup>K. Takada, H. Sakurai, E. Takayama-Muromachi, F. Izumi, R. A. Dilanian, and T. Sasali, Nature (London) **422**, 53 (2003).
- <sup>4</sup>B. C. Sales, R. Jin, K. A. Affholter, P. Khalifah, G. M. Veith, and D. Mandrus, Phys. Rev. B **70**, 174419 (2004).
- <sup>5</sup>T. Motohashi, R. Ueda, E. Naujalis, T. Tojo, I. Terasaki, T. Atake, M. Karppinen, and H. Yamauchi, Phys. Rev. B **67**, 064406 (2003).
- <sup>6</sup>C. Bernhard, A. V. Boris, N. N. Kovaleva, G. Khaliullin, A. V. Pimenov, L. Yu, D. P. Chen, C. T. Lin, and B. Keimer, Phys. Rev. Lett. **93**, 167003 (2004).
- <sup>7</sup>W. B. Wu, D. J. Huang, J. Okamoto, A. Tanaka, H.-J. Lin, F. C. Chou, A. Fujimori, and C. T. Chen, Phys. Rev. Lett. **94**, 146402 (2005).
- <sup>8</sup>G. Lang, J. Bobroff, H. Alloul, P. Mendels, N. Blanchard, and G. Collin, Phys. Rev. B **72**, 094404 (2005).
- <sup>9</sup>M. Daghofer, P. Horsch, and G. Khaliullin, Phys. Rev. Lett. **96**, 216404 (2006).
- <sup>10</sup>T. Kroll, M. Knupfer, J. Geck, C. Hess, T. Schwieger, G. Krabbes, C. Sekar, D. R. Batchelor, H. Berger, and B. Buchner, Phys. Rev. B **74**, 115123 (2006).
- <sup>11</sup>T. Kroll, A. A. Aligia, and G. A. Sawatzky, Phys. Rev. B **74**, 115124 (2006).
- <sup>12</sup>D. J. Singh, Phys. Rev. B **61**, 13397 (2000).
- <sup>13</sup>W. Koshibae and S. Maekawa, Phys. Rev. Lett. **91**, 257003 (2003).
- <sup>14</sup>M. D. Johannes, I. I. Mazin, D. J. Singh, and D. A. Papaconstantopoulos, Phys. Rev. Lett. **93**, 097005 (2004).
- <sup>15</sup>L.-J. Zou, J.-L. Wang, and Z. Zeng, Phys. Rev. B **69**, 132505 (2004).
- <sup>16</sup>Q.-H. Wang, D.-H. Lee, and P. A. Lee, Phys. Rev. B **69**, 092504 (2004).
- <sup>17</sup>K.-W. Lee, J. Kunes, and W. E. Pickett, Phys. Rev. B **70**, 045104 (2004).
- <sup>18</sup>P. Zhang, W. Luo, V. H. Crespi, M. L. Cohen, and S. G. Louie, Phys. Rev. B **70**, 085108 (2004).
- <sup>19</sup>F. C. Chou, J. H. Cho, and Y. S. Lee, Phys. Rev. B **70**, 144526 (2004).
- <sup>20</sup>H. Ishida, M. D. Johannes, and A. Liebsch, Phys. Rev. Lett. **94**, 196401 (2005).
- <sup>21</sup>S. Zhou, M. Gao, H. Ding, P. A. Lee, and Z. Wang, Phys. Rev. Lett. **94**, 206401 (2005).
- <sup>22</sup>F. Lechermann, S. Biermann, and A. Georges, Prog. Theor. Phys. **160**, 233 (2005).
- <sup>23</sup>S. Landron and M.-B. Lepetit, Phys. Rev. B **74**, 184507 (2006).
- <sup>24</sup>C. A. Marianetti and G. Kotliar, Phys. Rev. Lett. **98**, 176405 (2007).
- <sup>25</sup>M. M. Korshunov, I. Eremin, A. Shorikov, and V. I. Anisimov, JETP Lett. **84**, 650 (2007).
- <sup>26</sup>S. Landron and M.-B. Lepetit, Phys. Rev. B **77**, 125106 (2008).
- <sup>27</sup>D. Pillay, M. D. Johannes, I. I. Mazin, and O. K. Andersen, Phys. Rev. B **78**, 012501 (2008).
- <sup>28</sup>J. Carl, *Ballhausen: Introduction to Ligand Field Theory* (McGraw-Hill, United States of America, 1962), p.68.
- <sup>29</sup>G. J. Shu, Andrea Prodi, S. Y. Chu, Y. S. Lee, H. S. Sheu, and F. C. Chou, Phys. Rev. B **76**, 184115 (2007).
- <sup>30</sup>Y. Ihara, K. Ishida, H. Ohta, and K. Yoshimura, J. Phys. Soc. Jpn. **77**, 073702 (2008).
- <sup>31</sup>M. W. Haverkort, Z. Hu, J. C. Cezar, T. Burnus, H. Hartmann, M. Reuther, C. Zobel, T. Lorenz, A. Tanaka, N. B. Brookes, H. H. Hsieh, H.-J. Lin, C. T. Chen, and L. H. Tjeng, Phys. Rev. Lett. **97**, 176405 (2006).
- <sup>32</sup>Details concerning the XAS experiments on BaCoO<sub>3</sub> will be reported in a separate paper.
- <sup>33</sup>F. M. F. de Groot, J. Electron Spectrosc. Relat. Phenom. **67**, 529 (1994).
- <sup>34</sup>A. Tanaka and T. Jo, J. Phys. Soc. Jpn. **63**, 2788 (1994).
- <sup>35</sup>Z. Hu, Hua Wu, M. W. Haverkort, H. H. Hsieh, H.-J. Lin, T. Lorenz, J. Baier, A. Reichl, I. Bonn, C. Felser, A. Tanaka, C. T. Chen, and L. H. Tjeng, Phys. Rev. Lett. **92**, 207402 (2004).
- <sup>36</sup>S. I. Csiszar, M. W. Haverkort, Z. Hu, A. Tanaka, H. H. Hsieh, H.-J. Lin, C. T. Chen, T. Hibma, and L. H. Tjeng, Phys. Rev. Lett. **95**, 187205 (2005).
- <sup>37</sup>T. Burnus, Z. Hu, M. W. Haverkort, J. C. Cezar, D. Flahaut, V. Hardy, A. Maignan, N. B. Brookes, A. Tanaka, H. H. Hsieh, H.-J. Lin, C. T. Chen, and L. H. Tjeng, Phys. Rev. B **74**, 245111 (2006).
- <sup>38</sup>T. Burnus, Z. Hu, H. H. Hsieh, V. L. J. Joly, P. A. Joy, M. W. Haverkort, Hua Wu, A. Tanaka, H.-J. Lin, C. T. Chen, and L. H. Tjeng, Phys. Rev. B **77**, 125124 (2008).
- <sup>39</sup>T. Burnus, Z. Hu, Hua Wu, J. C. Cezar, S. Niitaka, H. Takagi, C. F. Chang, N. B. Brookes, H. J. Lin, L. Y. Jang, A. Tanaka, K. S. Liang, C. T. Chen, and L. H. Tjeng, Phys. Rev. B **77**, 205111 (2008).
- <sup>40</sup>C. F. Chang, Z. Hu, Hua Wu, T. Burnus, N. Hollmann, M. Benomar, T. Lorenz, A. Tanaka, H.-J. Lin, H. H. Hsieh, C. T. Chen, and L. H. Tjeng, Phys. Rev. Lett. **102**, 116401 (2009).
- <sup>41</sup>Q. Huang, M. L. Foo, R. A. Pascal, Jr., J. W. Lynn, B. H. Toby, Tao He, H. W. Zandbergen, and R. J. Cava, Phys. Rev. B **70**, 184110 (2004).
- <sup>42</sup>J. van Elp, J. L. Wieland, H. Eskes, P. Kuiper, G. A. Sawatzky, F. M. F. de Groot, and T. S. Turner, Phys. Rev. B **44**, 6090 (1991).
- <sup>43</sup>M. T. Czyzyk, R. Potze, and G. A. Sawatzky, Phys. Rev. B **46**, 3729 (1992).
- <sup>44</sup>M. Abbate, J. C. Fuggle, A. Fujimori, L. H. Tjeng, C. T. Chen, R. Potze, G. A. Sawatzky, H. Eisaki, and S. Uchida, Phys. Rev. B **47**, 16124 (1993).
- <sup>45</sup>M. Abbate, R. Potze, G. A. Sawatzky, and A. Fujimori, Phys. Rev. B **49**, 7210 (1994).
- <sup>46</sup>T. Saitoh, A. E. Bocquet, T. Mizokawa, and A. Fujimori, Phys. Rev. B **52**, 7934 (1995).
- <sup>47</sup>T. Mizokawa and A. Fujimori, Phys. Rev. B **53**, R4201 (1996).
- <sup>48</sup>T. Mizokawa and A. Fujimori, Phys. Rev. B **54**, 5368 (1996).
- <sup>49</sup>Priya Mahadevan, N. Shanthi, and D. D. Sarma, Phys. Rev. B **54**, 11199 (1996).
- <sup>50</sup>T. Saitoh, T. Mizokawa, A. Fujimori, M. Abbate, Y. Takeda, and M. Takano, Phys. Rev. B **55**, 4257 (1997).
- <sup>51</sup>Parameters (in units of eV):  $U_{dd}=5$ ,  $U_{dc}=6$ ,  $\Delta=4$  (for Co<sup>3+</sup>),  $\Delta=-1$  (for Co<sup>4+</sup>),  $V_{eg}=3.5$ . The Slater integrals were reduced to 80% and 60% of their Hartree-Fock values for Co<sup>3+</sup> and Co<sup>4+</sup>, respectively. See Ref. 34 for definitions.
- <sup>52</sup>Y. Kumagai, H. Ikeno, F. Oba, K. Matsunaga, and I. Tanaka, Phys. Rev. B **77**, 155124 (2008).
- <sup>53</sup>J. H. Park, L. H. Tjeng, A. Tanaka, J. W. Allen, C. T. Chen, P. Metcalf, J. M. Honig, F. M. F. de Groot, and G. A. Sawatzky, Phys. Rev. B **61**, 11506 (2000).
- <sup>54</sup>K. W. Blazey and K. A. Müller, J. Phys. C **16**, 5491 (1983).

- <sup>55</sup>H. Eskes, M. B. J. Meinders, and G. A. Sawatzky, *Phys. Rev. Lett.* **67**, 1035 (1991).
- <sup>56</sup>M. B. J. Meinders, H. Eskes, and G. A. Sawatzky, *Phys. Rev. B* **48**, 3916 (1993).
- <sup>57</sup>M. Z. Hasan, Y.-D. Chuang, D. Qian, Y. W. Li, Y. Kong, A. P. Kuprin, A. V. Fedorov, R. Kimmerling, E. Rotenberg, K. Rossnagel, Z. Hussain, H. Koh, N. S. Rogado, M. L. Foo, and R. J. Cava, *Phys. Rev. Lett.* **92**, 246402 (2004).
- <sup>58</sup>H.-B. Yang, Z.-H. Pan, A. K. P. Sekharan, T. Sato, S. Souma, T. Takahashi, R. Jin, B. C. Sales, D. Mandrus, A. V. Fedorov, Z. Wang, and H. Ding, *Phys. Rev. Lett.* **95**, 146401 (2005).
- <sup>59</sup>D. Qian, L. Wray, D. Hsieh, L. Viciu, R. J. Cava, J. L. Luo, D. Wu, N. L. Wang, and M. Z. Hasan, *Phys. Rev. Lett.* **97**, 186405 (2006).
- <sup>60</sup>J. Geck, S. V. Borisenko, H. Berger, H. Eschrig, J. Fink, M. Knupfer, K. Koepernik, A. Koitzsch, A. A. Kordyuk, V. B. Zabolotnyy, and B. Buchner, *Phys. Rev. Lett.* **99**, 046403 (2007).
- <sup>61</sup>C. T. Chen and F. Sette, *Phys. Scr.* **T31**, 119 (1990).
- <sup>62</sup>C. Mitra, Z. Hu, P. Raychaudhuri, S. Wirth, S. I. Csiszar, H. H. Hsieh, H.-J. Lin, C. T. Chen, and L. H. Tjeng, *Phys. Rev. B* **67**, 092404 (2003).